Electronic Supplementary Material (ESI) for Analytical Methods.

Electronic Supplementary Information

Mesoporous Pd@Pt core-shell nanoparticles supported on multi-walled carbon nanotubes as a sensing platform: Application to simultaneous electrochemical detection of anticancer drugs doxorubicin and dasatinib

Pramod K. Kalambate, Yankai Li, Yue Shen, Yunhui Huang*

State Key Laboratory of Materials Processing and Die & Mould Technology, School of Materials Science and Engineering, Huazhong University of Science and Technology, Wuhan, Hubei 430074, P. R. China

***Corresponding author:**

E-mail: huangyh@mail.hust.edu.cn

Tel: 86-027-87558237; Fax: 86-027-87558241

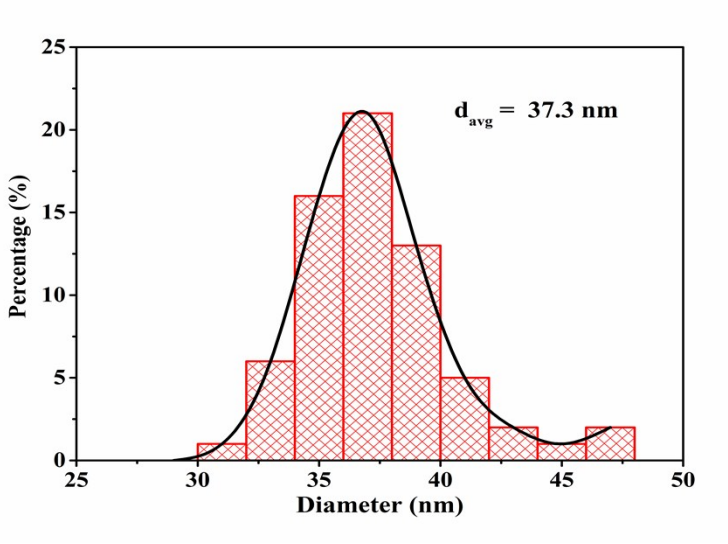

Fig. S1 Particle size distribution histogram obtained from TEM analysis

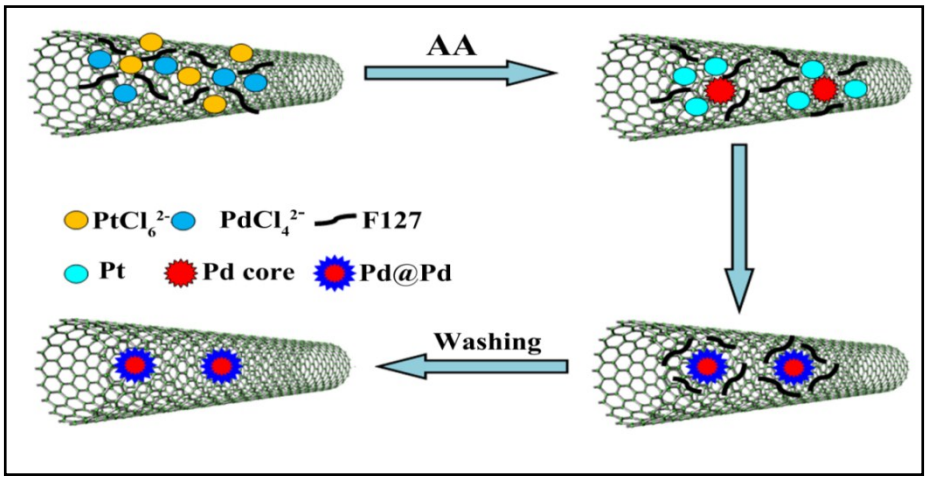

Fig. S2 The stepwise synthesis of Pd@Pt/MWCNT

1. Formation mechanism of Pd@Pt

The formation mechanism of Pd@Pt is illustrated in Fig. S2. The standard reduction potential of Pt ions $[PtCl6]^{2-}$ /Pt (0.76 V *vs*. SHE) is more positive than Pd ions $[PdCl_4]^{2-}$ (0.59V *vs.* SHE). So with this principle Pt precursor is expected to reduce first than Pd precursor and therefore the formation of Pd@Pt core-shell structure is unexpected. However, the only reason behind formation of Pd@Pt structure can be explained on the basis of difference in reduction rates of two metals (Pd reduction rate > Pt reduction rate). Such unusual behaviour is observed in previous studies for simultaneous reduction of Pd and Pt [1, 2]. Therefore, Pd precursor is reduced first by ascorbic acid forming a Pd seeds and then formation of Pt

nanoparticles on Pd forming a core-shell structure. During this process, F127 molecules are adsorbed on Pd seeds and act as a stabilizing agent. In the present case, the concentration of surfactant is over critical micelle concentration (CMC) forming the spherical micelles. During the growth of Pt on Pd seeds, F127 micelles interact with Pd seeds and acts as structure director forming Pd@Pt core-shell mesoporous structure

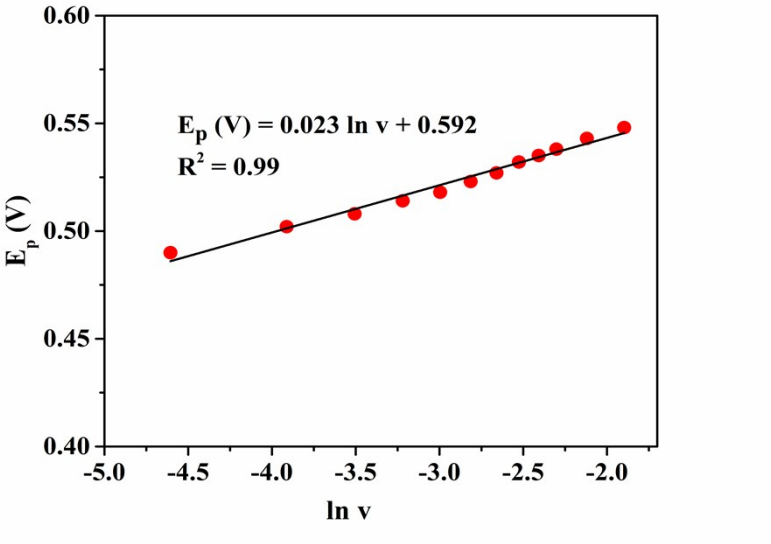

Fig. S3 Plot of E_p *vs*. ln *v* obtained from scan rate (V s^{-1}) of doxorubicin

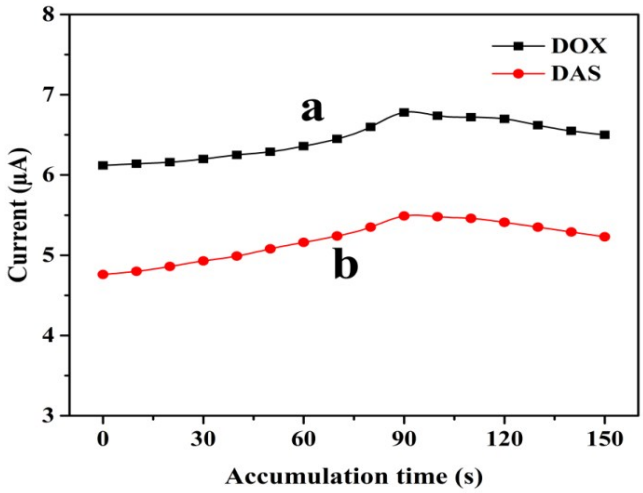

Fig. S4 Effect of accumulation time (t_{acc}) on peak current of (**a)** 2.4 µM DOX and (**b)** 3.0 µM DAS

2. Optimization of SWV parameters

The effect of accumulation time (t_{acc}) on peak currents of 2.4 μM DOX and 3.0 μM DAS was carefully studied in PBS (0.1M, pH 6.0) through SWV. The optimization was carried out in such a way that one parameter was changed while others were kept constant. Firstly, OCP was considered as E_{acc} at which maximum current response was obtained. Secondly, the effect of t_{acc} on peak currents was investigated in the range 0-150 s at OCP. As can be seen in Fig. S4 that with increase of the t_{acc} the peak currents increases up to 90 s and decreases afterwards may be due to the saturation at the electrode surface. Besides this, other operating parameters such as frequency (f), pulse amplitude (a) and scan increment (ΔE_s) were also explored in order to get maximum analytical signal and better peak separation. Hence, sensitive determination of DOX and DAS was performed by AdSSWV at E_{acc} = OCP, t_{acc} = 90 s, f = 5 Hz, a = 30 mV, ΔE_s = 4 mV and equilibrium time = 10 s.

Tables

Table S1 Analytical parameters for electrochemical determination of DOX and DAS in PBS (0.1 M, pH 6.0)

No.	Molecule	LWR (nM)	LRE	R^2	LOD (nM)
(A) Statistical data for individual molecules					
1	DOX	3.8-8410	I_p(μA)=0.021C (10^{-8} M) + 1.451	0.993	0.73
2	DAS	37-9720	I_p(μA)= 0.015 C(10^{-8}M) + 1.128	0.993	5.83
(B) Statistical data for DOX when the concentration of DAS is kept constant (4.1 μM)					
3	DOX	4.2-8520	I_p(μA)= 0.02 C (10^{-8}M) + 1.506	0.991	0.8
(C) Statistical data for DAS when the concentration of DOX is kept constant (2.4 μM)					
4	DAS	37.5-9820	I_p(μA)= 0.014 C(10^{-8}M) + 1.222	0.992	6.25
(D) Statistical data for DOX and DAS simultaneously					
5	DOX	4.4-8580	I_p (μA)=0.019 C(10^{-8}M) + 1.501	0.991	0.86
	DAS	38-9880	I_p (μA)=0.013 C(10^{-8}M) + 1.228	0.991	6.72

Table S2 Comparison of the proposed sensor with literature for the electrochemical determination of DOX and DAS

Molecule	Sensor	Technique	LOD	Analytical Range	References
	GQD	CV	0.016 μM	0.018~3.60 μM	[3]
DOX	OMWCNT	CV	9.4×10^{-3} μM	0.04~90 μM	[4]
	MWCNT/$CoFe_2O_4$/CPE	CV	10 pM	0.05~1150 nM	[5]
	Mg_2Al-Cl-LDHs	CV	0.02 nM	10.0~2110.0 nM	[6]
	Hg(Ag)FE	SWV	9.89 ng mL^{-1}	4.99~59.64 ng mL^{-1}	[7]
	MAb/GNP/TB Sol–Gel	CV	0.09 pg mL^{-1}	2.5~50.0 pg mL^{-1}	[8]
	MWNT-COOH	CV	10 ngmL^{-1}	0.02~1.28 mu gmL^{-1}	[9]
	GNP/RGD-MAP-C	CV	0.01μg/mL	0.5~1.0 μg/mL	[10]
	GNPs/HDT	CV	1.74×10^{-11} M^{-1}	1.0 ~160.0 pg mL^{-1}	[11]
	ds–DNA/Au	CV	1 pM	0.08~0.5 M	[12]
	Ferrofluid	CV	—	0.05~0.5 mgml^{-1}	[13]
	AgNPs–CDs–rGO/GCE	DPV	2 nM	0.01~2.5 μM	[14]
	ZnO/BMTFB/CPE	SWV	9 nM	0.07–500 μM	[15]
	Pd@Pt/MWCNT	AdSSWV	0.86 nM	4.4-8580 nM	This work#
	Pd@Pt/MWCNT	AdSSWV	0.73 nM	3.8-8410 nM	This work*
DAS	GCE	DPV	0.13 μM	0.20 - 2.00 μM	[16]
	Pt/MWCNTs- BMIHFP	SWV	1.0 μM	5.0-500 μM	[17]
	ZnO/BMTFB/CPE	SWV	0.5 μM	1.0–1200 μM	[15]
	Pd@Pt/MWCNT	AdSSWV	6.72 nM	38-9880 nM	This work#
	Pd@Pt/MWCNT	AdSSWV	5.83 nM	37-9720 nM	This work*

#: Simultaneous determination; *: Individual determination

Abbreviations: graphene quantum dots (GQD); oxidized multiwalled carbon nanotube (OMWCNT); magnetic graphene oxide grafted with chlorosulfonic acid (Fe_3O_4-GO-SO_3H); spinel-structured cobalt ferrite ($CoFe_2O_4$); carbon paste electrode (CPE); layered double hydroxides (LDHs); silver amalgam film electrode (Hg(Ag)FE); gold nanoparticles (GNPs); thiol base sol-gel (TBSol-Gel); carboxylated multiwalled carbon nanotubes (MWNT-COOH); glycine-aspartic acid (RGD); 1,6-hexanedithiol (HDT); double-stranded DNA (ds-DNA); magnetic nanoparticle colloidal suspension (Ferrofluid); 1-butyl-3-methylimidazolium hexafluoro phosphate (BMIHFP); carbon dots (CDs); 1-butyl-3-methylimidazolium tetrafluoroborate (BMTFB)

Table S3 Precision and Bias of assay for DOX and DAS by the proposed voltammetric procedure (n = 5)

Molecule	Concentration (taken) (10^{-7} M)	Concentration (found) (10^{-7} M)	Recovery (%) (n = 5)	Bias (%)	Precision % RSD (n = 5)
DOX	Intra - day				
	1.19	1.175	98.7	1.3	1.98
	Inter – day				
	2.38	2.34	98.3	1.7	2.24
DAS	Intra – day				
	1.33	1.31	98.5	1.5	1.96
	Inter – day				
	2.26	2.22	98.2	1.8	2.16

Table S4 Recovery studies for individual determination of DOX and DAS in urine and blood serum samples (n=5)

Sample	Drug	Spiked (10^{-7} M)	Detected (10^{-7} M)	Recovery (%) ±% RSD
Urine Sample 1	DOX	Not spiked	Not found	---
		0.42	0.414	98.57 ± 1.89
		0.76	0.75	98.68 ± 1.96
		1.28	1.272	99.37 ± 1.98
Urine Sample 2	DAS	Not spiked	Not found	---
		0.47	0.47	100.0 ± 1. 93
		0.72	0.714	99.17 ± 1.95
		1.18	1.17	99.15 ± 1.98
Serum Sample 1	DOX	Not spiked	Not found	---
		0.35	0.345	98.57 ± 1.90
		0.77	0.765	99.35 ± 2.06
		1.32	1.32	100.0 ± 1.98
Serum Sample 2	DAS	Not spiked	Not found	---
		0.38	0.376	98.94 ± 2.04
		0.65	0.651	100.15 ± 2.11
		1.12	1.12	100.00 ± 2.08

References

[1] L. Wang, Y. Nemoto and Y. Yamauchi, *J. Am. Chem. Soc*., 2011, **133**, 9674-9677.

[2] L. Wang and Y. Yamauchi, *J. Am. Chem. Soc*., 2010, **132**, 13636-13638.

[3] M. Hasanzadeh, N. Hashemzadeh, N. Shadjou, J. Eivazi-Ziaei, M. K. Jafari and A. Jouyban, *J. Mol. Liq*., 2016, **221**, 354-357.

[4] E. Haghshenas, T. Madrakian and A. Afkhami, *Anal. Bioanal. Chem*., 2016, **408**, 2577-2586.

[5] M. Taei, F. Hasanpour, H. Salavati and S. Mohammadian, *Microchim Acta*, 2016, **183**, 49-56.

[6] M. Taei, F. Hasanpour and E. Dehghani, *J. Taiwan Inst. Chem. Eng*., 2015, **54**. 183-190.

[7] O. Vajdle, J. Zbiljic, B. Tasic, D. Jovic, V. Guzsvany and A. Djordjevic, *Electrochim. Acta*, 2014, **132**, 49-57.

[8] B. Rezaei, N. Askarpour and A. A. Ensafi, *Talanta*, 2014, **119**, 164-169.

[9] S. Wang, Z. Huang, M. Liu and H. Ding, Sens. Lett. 2012, **10**, 117-121.

[10] T. H. Kim, W. A. El-Said, J. H. An and J. W. Choi, *Nanomedicine*, 2013, **9**, 336-344.

[11] P. F. Rezaei, S. Fouladdel, S. Cristofanon, S. M. Ghaffari, G. R. Amin and E. Azizi *Cytotechnology*, 2011, **63**, 503-512.

[12] B. P. Ting, J. Zhang, Z. Gao and J. Y. Ying, *Biosens Bioelectron*, 2009, 25, 282-287.

[13] M. Brzozowska, P. Krysinski, *Electrochim. Acta*, 2009, **54**, 5065-5070.

[14] H. Guo, H. Jin, R. Gui, Z. Wang, J. Xia and F. Zhang, *Sens. Actuators, B,* 2017, **253**, 50–57.

[15] S. A. R. Alavi-Tabari, M. A. Khalilzadeh, H. Karimi-Maleh, *J. Electroanal. Chem*., 2018, **811**, 84-88.

[16] C. S. H. Jesus and V. C. Diculescu, *J. Electroanal. Chem*., 2015, **752**, 47–53.

[17] H. Karimi-Maleh, A. F. Shojaei, K. Tabatabaeian, F. Karimi, S. Shakeri and R. Moradi, *Biosens. Bioelectron*., 2016, **86**, 879–884.